Bolaños-Jiménez, R., Sevilla, A. & Martínez-Bazán, C. (2016, junio). Modeling of the bubbling process in a planar co-flow configuration. International Journal of Multiphase Flow, 82, 86-92.

DOI: 10.1016/j.ijmultiphaseflow.2016.02.010

Modeling of the bubbling process in a planar co-flow configuration

R. Bolaños-Jiménez,[1,*] A. Sevilla,[2,†] and C. Martínez-Bazán[1,‡]

[1] *Área de Mecánica de Fluidos, Departamento de Ingeniería Mecánica y Minera. Universidad de Jaén. Campus de las Lagunillas, 23071, Jaén, Spain.*

[2] *Área de Mecánica de Fluidos. Departamento de Ingeniería Térmica y de Fluidos. Universidad Carlos III de Madrid, 28911 Leganés, Spain*

Abstract

This work presents an analytical model developed to describe the bubbling regime resulting from the injection of an air sheet of thickness $2H_o$ with a velocity u_a between two water streams of thickness $H_w - H_o$, moving at a velocity u_w. Based on previous experimental and numerical characterizations of this flow, the gas stream is modeled as a two-dimensional sheet divided into three different parts in the streamwise direction: a neck that moves downstream at the water velocity, a gas ligament attached to the injector upstream of the neck, and a forming bubble downstream of the neck, whose uniform dimensionless half-thicknesses are $\eta_n(\tau)$, $\eta_l(\tau)$, $\eta_b(\tau)$ respectively, and the corresponding pressures are given by $\Pi_n(\tau)$, $\Pi_l(\tau)$, and $\Pi_b(\tau) = \Pi_n(\tau)$. Lengths are made dimensionless with the semi thickness of the air layer at the nozzle exit, H_o, and pressures with twice the air dynamic pressure, $\rho_a u_a^2$. In a reference frame moving with the water velocity, and imposing a negative pressure caused by the sudden expansion of the air stream at the outlet of the injector, a set of algebraic-differential equations are deduced, that can be numerically integrated to obtain the temporal evolution of the interface positions and gas pressures, as well as of the gas flow rate through the neck. The results provided by the model show a good agreement with previous experimental and numerical results for a given value of the initial velocity of the collapsing neck. The latter is the only free parameter of the model, that is shown to depend on the Weber number, $We = \rho_w u_w^2 H_o/\sigma$, and barely depends on the water-to-air velocity ratio, $\Lambda = u_w/u_a$, being σ is the surface tension coefficient.

*Electronic address: rbolanos@ujaen.es

†Electronic address: asevilla@ing.uc3m.es

‡Electronic address: cmbazan@ujaen.es

I. INTRODUCTION

Generation of gas bubbles in a liquid is one of the most important and common operations in many industrial applications, such as aeration, distillation, or absorption, traditionally used in material, mineral, chemical or food industries, among many others. In addition, in the last few years, a number of emerging technologies related with the medical and the pharmaceutical industries demand the generation of small monodisperse bubbles, justifying the need of a deeper understanding of the bubble size control[18]. The simplest and most studied method to generate bubbles consists of introducing the gas stream through an injector which discharges inside a still liquid medium (see [2,4,11–13,16], among others). However, this method only allows the controlled production of bubbles at frequencies much smaller, and bubble sizes much larger, than those required by most of the modern applications mentioned above.

One of the most extended methods to generate smaller and monodisperse bubbles is the well-known *co-flow* technique, where the gas discharges inside a laminar stream of liquid which flows in the same direction. This configuration allows to inject higher gas flow-rates compared to the case of still liquid, while avoiding bubble coalescence and irregular bubbling regimens. The classical co-flow configuration with a cylindrical geometry has been extensively studied and it is used in many applications[3,6,14,16,19–21], including microfluidic devices[5,6,22]. Nevertheless, a planar co-flow configuration, which is the case studied in the present work, represents an alternative method to produce controlled-size bubbles[1,9,10]. In this configuration, which has been comparatively less studied than the cylindrical one, a planar air film discharges between two parallel water sheets. As in the cylindrical case, Bolaños *et al.*[1] observed the existence of two different flow regimes: a *jetting regime*, where the air sheet does not break near the injector, and a *bubbling regime*, where a periodic and quasi-two-dimensional break-up of the air sheet into individual bubbles is observed (see Fig. 1a). In addition, they characterized the jetting-to-bubbling transition in the $\mathrm{We} - \Lambda$ parameter space where $\mathrm{We} = \rho_w \, u_w^2 H_o/\sigma$ is the Weber number and $\Lambda = u_w/u_a$ the liquid-to-gas mean velocity ratio. Here, ρ_w is the water density, σ the surface tension coefficient, and H_o the half-thickness of the air stream at the exit slit (see Fig. 1b). Unlike in the cylindrical configuration where surface tension effects contribute to destabilizing the air-water jet[21], they stabilize the water-air-water sheet in the planar case. Moreover, a local linear stability analysis revealed that the flow transition is

related to the convective or absolute nature of the local instability in the near field.

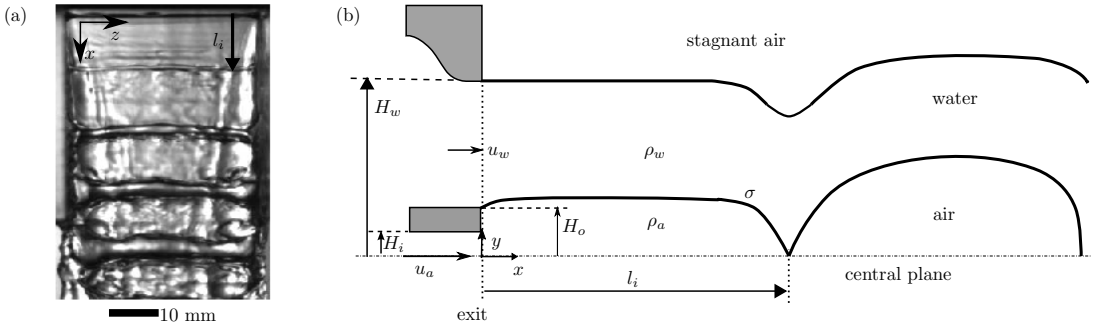

FIG. 1: (a) Experimental image of the bubbling regime in the planar co-flow configuration. (b) Sketch of the planar bubbling process with the main geometrical and physical parameters.

The dynamics of the bubbling regime in the planar configuration was also investigated by Gutiérrez-Montes *et al.*[9] by means of experiments and numerical simulations for a particular case with prescribed values of the dimensionless geometrical parameters, $h = H_w/H_o$ and $\beta = H_i/H_o$, where H_w is the distance of the water interface to the central plane, H_i and H_o the inner and outer semi thicknesses of the air injector respectively being, thus, $H_o - H_i$ the wall thickness of the air injector (see Fig. 1b). Based on the temporal evolution of the bubble shape and the gas pressure extracted from the numerical simulations performed by Gutiérrez-Montes *et al.*[9], the bubble formation event was described as a two-stage process: the *neck formation* and the subsequent *neck collapse* stages. The former starts just after the pinch-off of the previous bubble, when an initial air lump of length l_i, called *intact ligament*, remains attached to the outer wall of the air nozzle (see Fig. 1). Therefore, the gas stream suffers a sudden expansion from the inner thickness of the air injector, $2H_i$, to the outer one, $2H_o$, inducing a persistent negative gauge pressure inside the air stream in the neighborhood of the injector exit. As a consequence, an incipient neck appears, that propagates downstream at the water velocity while it accelerates inwards, causing a pressure drop across it. Thus, in order to keep the feeding air flow rate constant, the gas pressure at the exit has to increase. This process continues in time and during the *collapse stage* it becomes more violent, inducing the inflation of the air ligament upstream from the neck and, consequently, decreasing the air flow rate that passes through the neck.

Based on the above description, Gutiérrez-Montes *et al.*[9] proposed a scaling law for the

characteristic bubbling time, given by $t_c = H_o/u_a\sqrt{(\rho_w/\rho_a)(h-1)/[\beta(1-\beta)]}$, which was shown to describe fairly well the experimental and numerical bubbling times. In this scaling law, the pressure loss associated with the planar sudden expansion is the only mechanism taken into account to cause the pressure decrease at the injector tip. However, in the cases where the relative wall thickness is very small, $1-\beta \ll 1$, when the effect of the sudden expansion is not dominant, alternative phenomena leading to negative gauge pressures in the air stream determine the bubbling time, such as the Bernoulli suction through the neck (Venturi effect) or the elongation of the growing bubble, as already pointed out in[9,10]. Regarding the Bernoulli suction, although it is dominant during the last instants of the bubble collapse, it can not account for the neck formation stage, as happens in the cylindrical configuration[7,8,20]. Concerning the elongation of the forming bubble, in[9] it was already elucidated that a negative pressure is only possible when the length of the forming bubble increases with time, in contrast with the cylindrical case[7]. The relative importance of the different suction mechanisms mentioned above depends on the specific geometry of the bubble, cylindrical or planar, and on details of the injection system, such as the thickness of the walls separating the air and water streams at the nozzle exit.

The main goal of the present work is to extend the theoretical understanding of the planar bubbling regime. To that end, we propose a simple analytical model incorporating the main physical mechanisms that determine the bubbling process at constant gas flow rate. In contrast with most of the previous efforts to model the bubbling phenomenon, which are based on global force balances[3,4,12,15,17,23,24], our approach is similar to that developed in[7] for the cylindrical case.

The work is organized as follows. The analytical model is described in detail in Section II, while an evaluation the model, including comparisons with experimental and numerical results, is shown in Section III. Finally, Section IV summarizes the main conclusions.

II. MODEL DESCRIPTION

To model the bubbling process, and based on the information extracted from previous experiments and numerical simulations, the simplified flow configuration sketched in Fig. 2

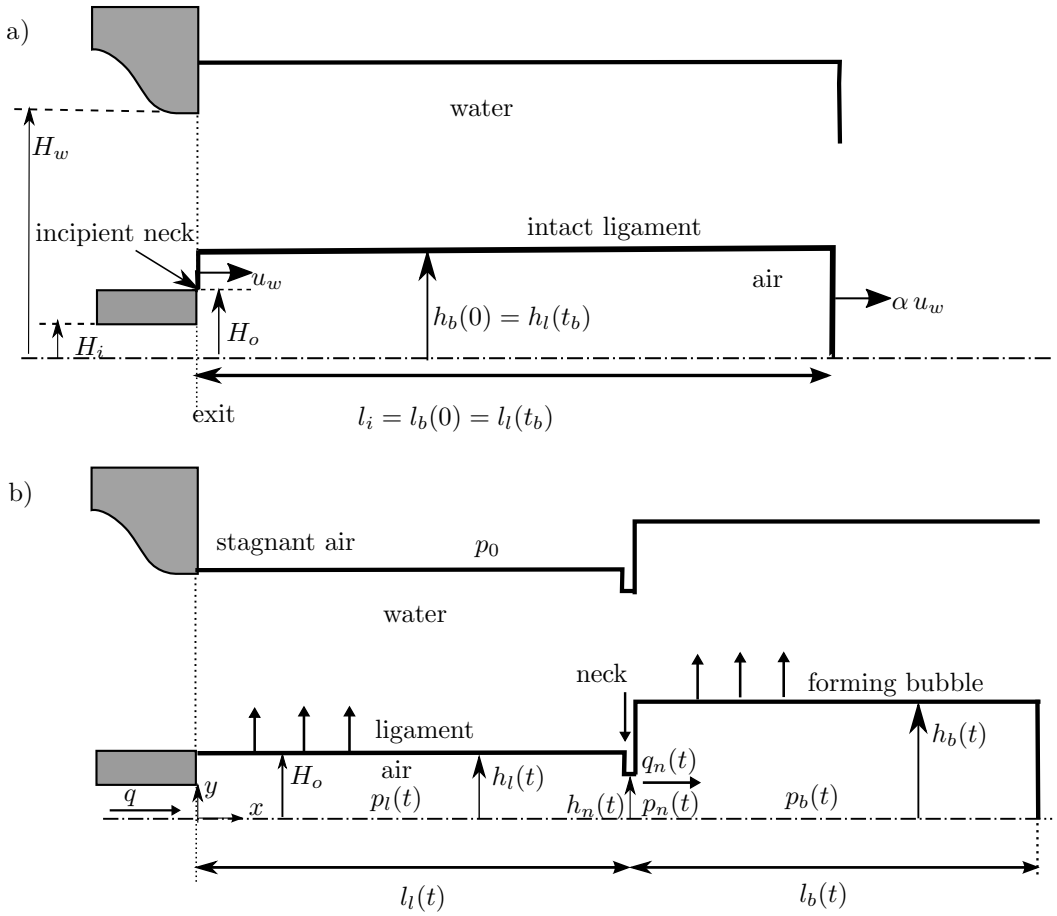

FIG. 2: Sketch of the bubble formation process showing the main variables included in the model. a) At the initial instant, $t = 0$, the length of the intact ligament is equal to the initial length of the forming bubble. b) For a generic instant, the air-water interface has been divided into three parts: ligament, neck, and forming bubble.

will be considered. For a generic instant t (Fig. 2b), the gas stream is modeled as a planar sheet divided into three different parts with uniform thicknesses and pressures: a contraction region at the *neck* of negligible length, with half-thickness $h_n(t)$ and pressure $p_n(t)$; a *ligament* upstream from the neck, with half-thickness $h_l(t)$, length $l_l(t)$ and pressure $p_l(t)$; and a *forming bubble* downstream from the neck, with half-thickness $h_b(t)$, length $l_b(t)$ and pressure $p_b(t)$. As already mentioned, since the air interface attaches to the outer edge of the injector wall, a negative pressure is established when the air discharges inside the bubble. Consequently, the air-water interface can not expand in the neighborhood of the injector, and since the growing bubble is inflated, an neck starts to form at the injector tip (Fig. 2a). As time evolves, the neck propagates downstream while it begins to close since $p_n(t) < p_0$, decreasing its thickness

$h_n(t)$, and generating a local pressure drop in the gas stream, as it occurs across a closing valve. Furthermore, on the one hand, to satisfy the condition of constant feeding air flow rate, q, the pressure inside the ligament, p_l, has to increase to compensate for such pressure drop. On the other hand, the neck pressure decreases due to the Venturi effect caused by the acceleration of gas stream. This overpressure causes the ligament to inflate, reducing the gas flow through the neck, $q_n(t)$, injected into the forming bubble. This phenomenon is more pronounced as the neck closes since the pressure drop is higher. Finally, the neck collapses, forming a new bubble and starting a new event. Thus, at the beginning of the process, $t = 0$, just after the detachment of the previous bubble (Fig. 2a), an intact air ligament of length l_i and semi-thickness $h_b(0) \gtrsim H_o$ remains attached to the needle. As shown in Fig. 2a, due to the periodicity of the bubble formation phenomenon, the shape of the intact ligament satisfies the conditions $h_b(0) = h_l(t_b)$, and $l_b(0) = l_l(t_b)$, where t_b is the bubble generation time.

Since the propagation velocity of the neck is approximately equal to the water velocity[9], to develop the model we will adopt a reference frame moving with velocity u_w. Consequently, the velocity of the gas stream injected through the nozzle is $(u_a - u_w)$ and the length of the ligament can be expressed as $l_l(t) = u_w t$. In addition, we will take into account the fact that the tip of the bubble may move slightly faster than the neck, considering that $l_b(t) = l_i + (\alpha - 1)u_w t$, with $\alpha \geq 1$.

To develop the model we will apply the conservation equations in the water stream around the three parts of the bubble defined above: neck, ligament and forming bubble. Notice that, in the moving reference frame defined above, in a first approximation, the water stream has only a transverse velocity component, v_w. The continuity equation applied to the water stream *around the neck region* provides,

$$\frac{\partial v_w}{\partial y} = 0 \rightarrow v_w = C(t) = \dot{h}_n(t)\,, \tag{1}$$

where the dot indicates time derivatives. Taking into account that $\mathrm{Re}_w \gg 1$, the transverse momentum equation gives

$$\rho_w\, \ddot{h}_n = -\frac{\partial p_w}{\partial y}\,, \tag{2}$$

with initial conditions $h_n(0) = H_o$ and $\dot{h}_n(0) = 0$, although the latter condition must be modified to properly account for the experimental results, as explained in detail later on. Equation (2) can be integrated across the water sheet, providing the following Rayleigh-

Plesset-like equation that models the dynamics of the planar liquid stream during the collapse of the neck,

$$\rho_w \ddot{h}_n \, (h_w - h_n) = p_w(h_n) - p_w(h_w) \, . \tag{3}$$

In the following we will consider that the water layer thickness is constant, and therefore $h_w - h_n = H_w - H_o$, an that the liquid Weber number is sufficiently large to neglect surface tension effects. Consequently, $p_w(h_n) = p_n$ and $p_w(h_w) = p_0$, with p_0 the atmospheric pressure. Equation (3) can be rearranged as

$$\ddot{h}_n = \frac{p'_n}{\rho_w \, H_o \, (h-1)}, \tag{4}$$

where $h = H_w/H_o$ is the water-to-air thickness ratio, and $p'_n(t) = p_n(t) - p_0$ is the manometric pressure inside the neck. Note that, for consistency with our previous works, h is a dimensionless geometrical parameter that should not be confused with any of the time dependent bubble thicknesses, $h_n(t)$, $h_l(t)$, and $h_b(t)$. Here, $p'_n(t)$ can be expressed in terms of a dynamic contribution, $p'_{nd}(t)$, and a constant negative pressure caused by the sudden planar expansion of the air stream, $-\rho_a \, u_a^2 \, \beta(1-\beta)$, as

$$p'_n = p'_{nd}(t) - \rho_a \, u_a^2 \, \beta(1-\beta), \tag{5}$$

where $\beta = H_i/H_o$ is the inner-to-outer thickness ratio of the air injector.

Similarly, if the continuity and momentum equations are applied to the water stream in a region around the ligament, the acceleration of the ligament is given by,

$$\ddot{h}_l = \frac{p'_l}{\rho_w \, H_o \, (h-1)}, \tag{6}$$

where the manometric pressure inside the air ligament, p'_l, can also be expressed as a temporally evolving contribution and a constant negative pressure,

$$p'_l = p'_{ld}(t) - \rho_a \, u_a^2 \, \beta(1-\beta). \tag{7}$$

Finally, for the water stream surrounding the forming bubble we can obtain the transverse acceleration of the bubble interface,

$$\ddot{h}_b = \frac{p'_n}{\rho_w \, H_o \, (h-1)}, \tag{8}$$

where it has been taken into account that the pressure inside the forming bubble is equal to the pressure in the neck, $p_b = p_n$, since the air discharges into the forming bubble through

the neck as a submerged jet. Therefore, considering Eqs. (3) and (6), in our simple model the accelerations of the neck and bubble interfaces must be the same,

$$\ddot{h}_n = \ddot{h}_b. \tag{9}$$

Moreover, assuming that the gas flowing from the ligament to the neck is quasi-steady and incompressible, the pressure inside the neck, p'_n, can be related to that of the ligament, p'_l, applying the Bernoulli's equation to an air streamline from the ligament to the neck,

$$p'_l + \frac{1}{2}\rho_a \frac{{q_n^*}^2}{{h_l}^2} = p'_n + \frac{1}{2}\rho_a \frac{{q_n^*}^2}{{h_n}^2}, \tag{10}$$

where q_n^* is the gas flow rate through the neck, defined as $q_n^* = Q_n/(2b)$, being b the spanwise length. The gas flow rate through the neck can be related with the geometry of the forming bubble through the continuity equation, $q_n^* = dV_b/dt$, where $V_b(t) = l_b(t)\, h_b(t)$ is the bubble volume per spanwise length, and $l_b = (\alpha - 1)u_w\, t + l_i$ is the instantaneous length of the bubble,

$$q_n^* = l_b\, \dot{h}_b + \dot{l}_b\, h_b = [(\alpha - 1)u_w t + l_i]\, \dot{h}_b + (\alpha - 1)u_w\, h_b. \tag{11}$$

In addition, q_n^* can also be expressed applying the continuity equation to the ligament,

$$q_n^* = q^* - dV_l/dt = q^* - \, u_w(\dot{h}_l\, t + h_l), \tag{12}$$

where q^* is the injected gas flow rate and $V_l(t) = l_l(t)\, h_l(t)$ is the volume of the ligament and $l_l(t) = u_w t$. The continuity equation can also be applied to the total gas volume, $V_t = V_l + V_b$, providing $q^* = dV_t/dt$,

$$q^* = u_w[h_l + \dot{h}_l\, t + (\alpha - 1)(h_b + \dot{h}_b\, t)] + \dot{h}_b\, l_i. \tag{13}$$

Since the feeding gas flow rate q^* is constant, $dq^*/dt = 0$, the time derivative of Eq. (13) gives,

$$0 = u_w\, [2\, \dot{h}_l + \ddot{h}_l\, t + (\alpha - 1)(2\dot{h}_b + \ddot{h}_b\, t)] + \ddot{h}_b\, l_i. \tag{14}$$

Introducing the dimensionless variables $S = \rho_a/\rho_w$, $\beta = H_i/H_o$, $\Lambda = u_w/u_a = H_i\, u_w/q^*$, $h = H_w/H_o$, $\eta_n(\tau) = h_n/H_o$, $\eta_l(\tau) = h_l/H_o$, $\eta_b(\tau) = h_b/H_o$, $L_i = l_i/H_o$, $\Pi_n(\tau) = p'_n/(\rho_a\, u_a^2)$, $\Pi_l(\tau) = p'_l/(\rho_a\, u_a^2)$ and $\tau = t\, u_w/H_o$, Eq. (4) becomes

$$\ddot{\eta}_n = \frac{S}{2\,\Lambda^2(h-1)}\left[\Pi_n(\tau) - \gamma_n\, \beta(1-\beta)\right], \tag{15}$$

with the initial conditions $\eta_n(0) = 1$ and $\dot{\eta}_n(0) = 0$, where the value of the latter will be discussed later on. As discussed below, in Eq. (15) we have introduced a parameter γ_n that

allows us to neglect the pressure loss due to the sudden expansion in the neck setting $\gamma_n = 0$.

Similarly, the dimensionless counterpart of Eq. (6) writes,

$$\ddot{\eta}_l = \frac{S}{2\,\Lambda^2(h-1)}\left[\Pi_l(\tau) - \gamma_l\,\beta(1-\beta)\right], \tag{16}$$

with $\eta_l(0) = 1$ and $\dot{\eta}_l(0) = 0$. The parameter γ_l plays the same role in Eq. (16) as γ_n in Eq. (15). The parameters γ_l and γ_n have been introduced because the model for simplicity does not contemplate spatial pressure variations inside the gas pocket, and thus is not able to consider the pressure loss $-\beta(1-\beta)$ in the neck and in the ligament simultaneously. In particular, if $\gamma_l = \gamma_n = 1$, the continuity equation can not be satisfied. Moreover, the dimensionless acceleration of the interface of the forming bubble writes,

$$\ddot{\eta}_b = \ddot{\eta}_n, \tag{17}$$

with $\eta_b(0) = \eta_{b,0}$ and $\dot{\eta}_b(0) = [\beta/\Lambda - 1 - (\alpha-1)\,\eta_{b,0}/L_i$ given by Eq. (13), where the dimensionless intact length is equal to the dimensionless bubbling time, $L_i = \tau_b$, provided that the neck moves downstream at the water velocity[9,10].

Equations (15)–(17) can be integrated to obtain the temporal evolution of $\eta_n(\tau)$, $\eta_l(\tau)$ and $\eta_b(\tau)$ if expressions for the dimensionless pressures $\Pi_l(\tau)$ and $\Pi_n(\tau)$ are found. On the one hand, using Eq. (10), Π_l can be obtained as a function of Π_n,

$$\Pi_l = \Pi_n - \frac{\Lambda^2}{2}\,q_n^2\left(\frac{1}{\eta_l^2} - \frac{1}{\eta_n^2}\right), \tag{18}$$

where q_n is the dimensionless gas flow rate given by the dimensionless counterpart of Eq. (11),

$$q_n = \frac{q_n^*}{u_w\,H_o} = (\alpha-1)(\eta_b + \dot{\eta}_b\tau) + \dot{\eta}_b\,L_i. \tag{19}$$

On the other hand, the dimensionless counterpart of Eq. (14) provides the closure to determine Π_n,

$$0 = 2\dot{\eta}_l + \ddot{\eta}_l\tau + 2(\alpha-1)\dot{\eta}_b + \ddot{\eta}_b[(\alpha-1)\tau + L_i]. \tag{20}$$

Introducing the expressions of $\ddot{\eta}_b$ and $\ddot{\eta}_l$ given by Eqs. (15)–(17) in Eq. (20) one gets,

$$\begin{aligned} 0 = {} & 2[(\alpha-1)\dot{\eta}_b + \dot{\eta}_l] + \frac{S}{2\,\Lambda^2(h-1)} \\ & \left\{\tau[\Pi_l - \gamma_l\,\beta(1-\beta)] + [(\alpha-1)\tau + L_i][\Pi_n - \gamma_n\,\beta(1-\beta)]\right\}. \end{aligned} \tag{21}$$

Finally, Π_n is obtained by substituting Eq. (18) into Eq. (21),

$$\Pi_n = \frac{\gamma_n\,\beta(1-\beta)[L_i+(\alpha-1)\tau] - \frac{4(h-1)\Lambda^2}{S}[\dot{\eta}_l+(\alpha-1)\dot{\eta}_b] + \gamma_l\,\beta(1-\beta)\tau + \\ + \frac{\Lambda^2\tau}{2}q_n^2\left[\frac{1}{\eta_l^2}-\frac{1}{\eta_n^2}\right]}{L_i+\alpha\,\tau}. \tag{22}$$

III. RESULTS

Equations (15)–(17) can be integrated together with Eqs. (18) and (22) to obtain the temporal evolutions of η_l, η_n, η_b, Π_l and Π_n. To that end, for an air-water system, $S = 1.2\times10^{-3}$, and a given geometry with $\beta = 5.27$ and $h = 0.52$, for any pair of We and Λ, an initial value of L_i must be provided to start an iterative computation of the periodic bubbling process, that converges when the length of the intact ligament, L_i, varies less than a given tolerance in two consecutive iterations. A value of $\alpha \simeq 1.1$ was prescribed according to our previous experimental and numerical results for all the cases explored in this work. Finally, the initial thickness of the forming bubble, $\eta_{b,0}$, was extracted from the numerical simulations. The model converges to a final result when $\eta_{b,0} = \eta_l(\tau_b)$ and $L_i = \tau_b$, being τ_b the bubbling time determined when the neck collapses, i.e. $\eta_n(\tau_b) = 0$.

To validate the model, we selected the case corresponding to $We = 38.26$ and $\Lambda = 0.145$, for which the experimental bubbling frequency given by Gutiérrez-Montes et al. [9] is $f_b = 207.4$ Hz. The results obtained from the model with $\gamma_n = 1$ and $\gamma_l = 0$ and initial neck velocity $\dot{\eta}_n$=0 are shown in Fig. 3. Notice that the final thickness of the ligament is equal to the initial thickness of the forming bubble, $\eta_b(0) = \eta_{b,0} = \eta_l(\tau_b) = 1.84$, indicating that the iterative process has converged. It can be observed that the temporal evolutions of $\eta_n(\tau)$, $\eta_l(\tau)$ and $\eta_b(\tau)$ provided by the model are consistent with the qualitative description of the bubbling process explained above. Indeed, as seen in Fig. 3(a), while the neck collapses the ligament and the forming bubble inflate with time. In addition, Fig. 3(b) shows that the pressure in the ligament, Π_l, increases, whereas the pressure inside the neck, Π_n, decreases with time. In particular, during the initial instants the pressure in the neck is $\Pi_n \simeq -0.05$, as can be seen more clearly in the inset of Fig. 3(b), and decreases with time due to the Venturi effect, which becomes especially pronounced towards the final instants of the necking process, $\tau > 42$. Furthermore, the flow rate of gas across the neck, q_n, decreases with time until it becomes zero

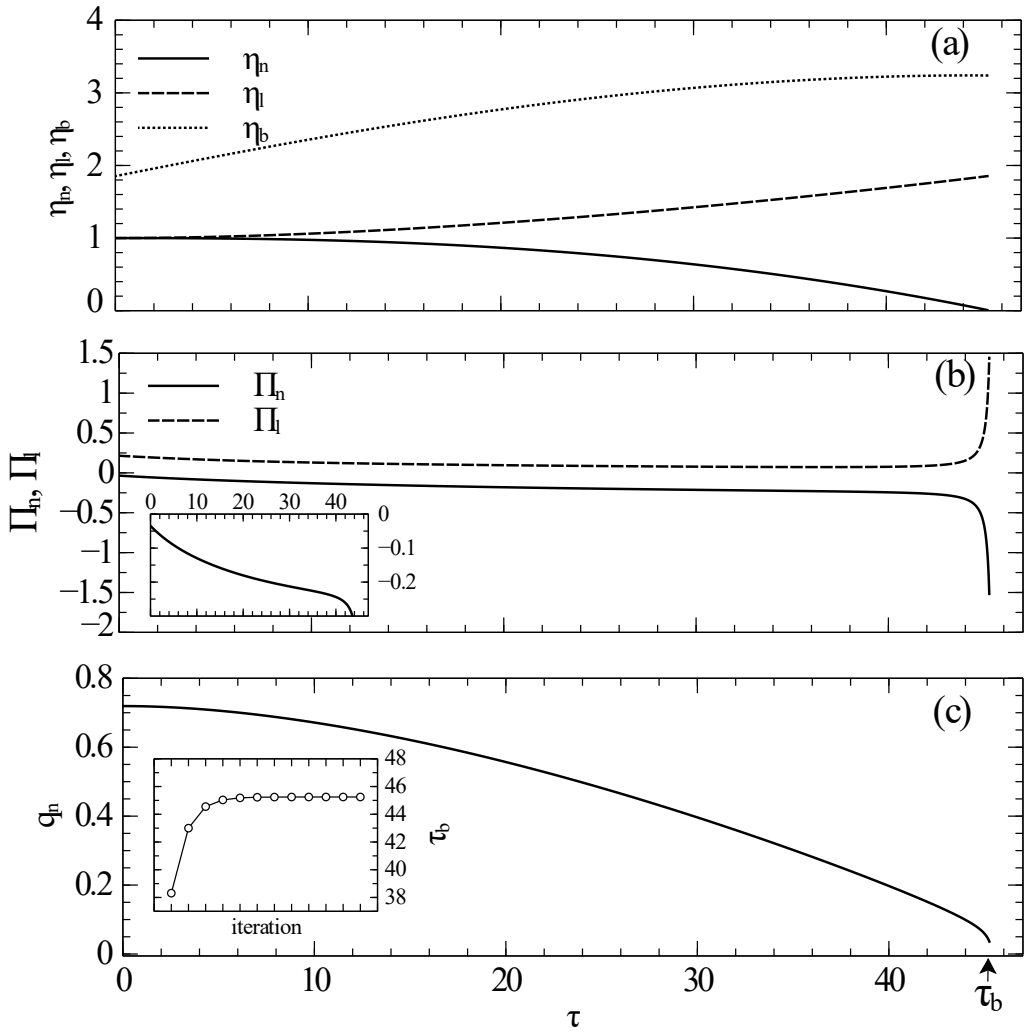

FIG. 3: Temporal evolution of a) the three parts of the gas dimensionless interface, ligament, neck and bubble; b) the gas dimensionless pressure inside the ligament and the neck; and c) the dimensionless gas flow through the neck, obtained from the model for $\beta = 0.52$, $h = 5.27$, $We = 38.26$, $\Lambda = 0.145$, $S = 1.2 \times 10^{-3}$, $\alpha = 1.1$, $\gamma_n = 1$, $\gamma_l = 0$ and $\dot{\eta}_n(0) = 0$. The inset in panel (b) is a zoom of the pressure in the neck, Π_n, showing that it is negative during the bubbling process. The inset in panel (c) shows the values of the bubbling time provided in each iteration, τ_b, indicating that model has converged.

when the bubble pinches off (see Fig. 3c). The inset in Fig. 3(c) shows how the bubbling time provided in each iteration, τ_b, quickly converges to the final value. However, in this case where the initial velocity of the neck was taken $\dot{\eta}_n$=0, the model converges to a initial thickness of the forming bubble and a bubbling time $\eta_l(\tau_b) = \eta_b(0) = 1.85$, $\tau_b = 45.25$, respectively,

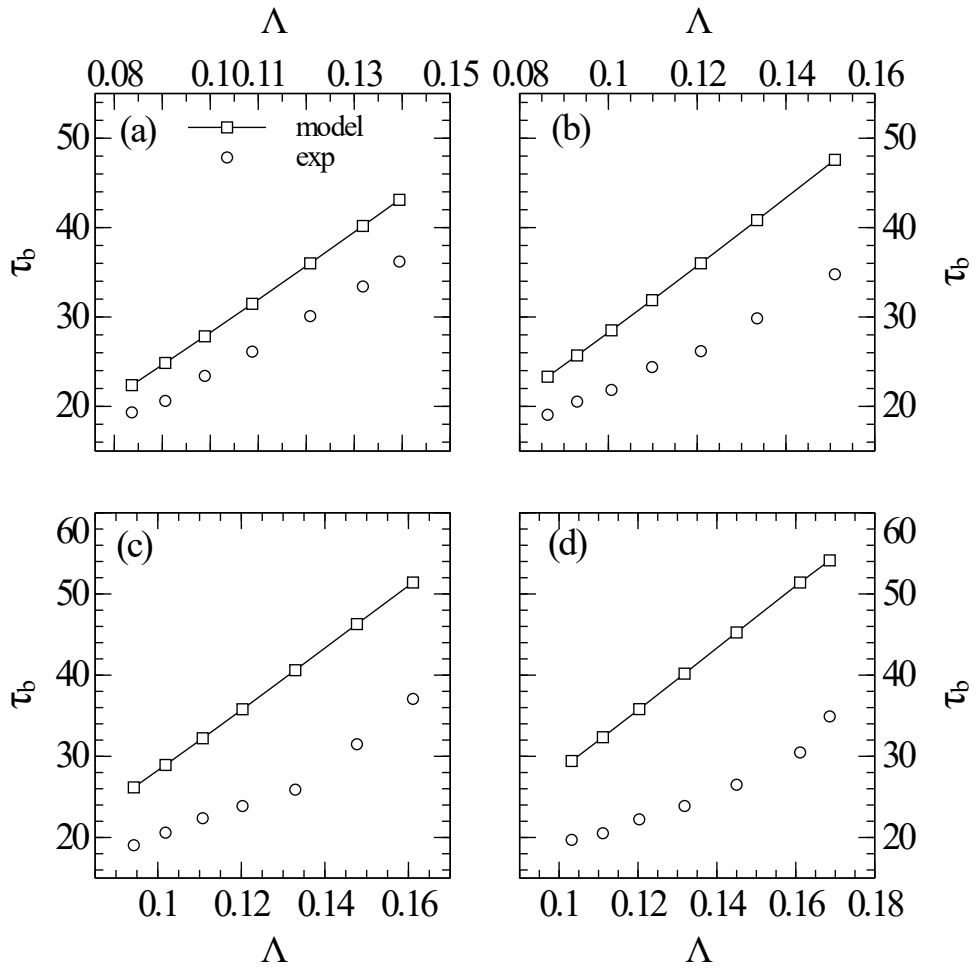

FIG. 4: Evolution of the dimensionless bubbling time, with the velocity ratio for different values of the Weber number, namely (a) $We = 21.52$, (b) $We = 26.57$, (c) $We = 32.15$, and (d) $We = 38.26$. Squares represent the solutions provided by the model with $\dot{\eta}_n(0)$=0 and the circles are the experimental values reported by Gutiérrez-Montes et al.[9]

being the latter much higher than the experimental value $\tau_b^{exp} = u_w/(H_o f_b) \simeq 27$ according to Gutiérrez-Montes et al.[9].

Following the same procedure, the model was integrated for different values of u_a and u_w, i.e different values of the Weber number and the air-to-water velocity ratio, also considering $\dot{\eta}_n(0)= 0$ as initial neck velocity. Figure 4 shows the dependence of the dimensionless bubbling time with the velocity ratio for different values of the Weber number, together with the experimental results. As can be observed, the bubbling times provided by the model follow the same behavior as those obtained experimentally, exhibiting and increase of τ_b with Λ with

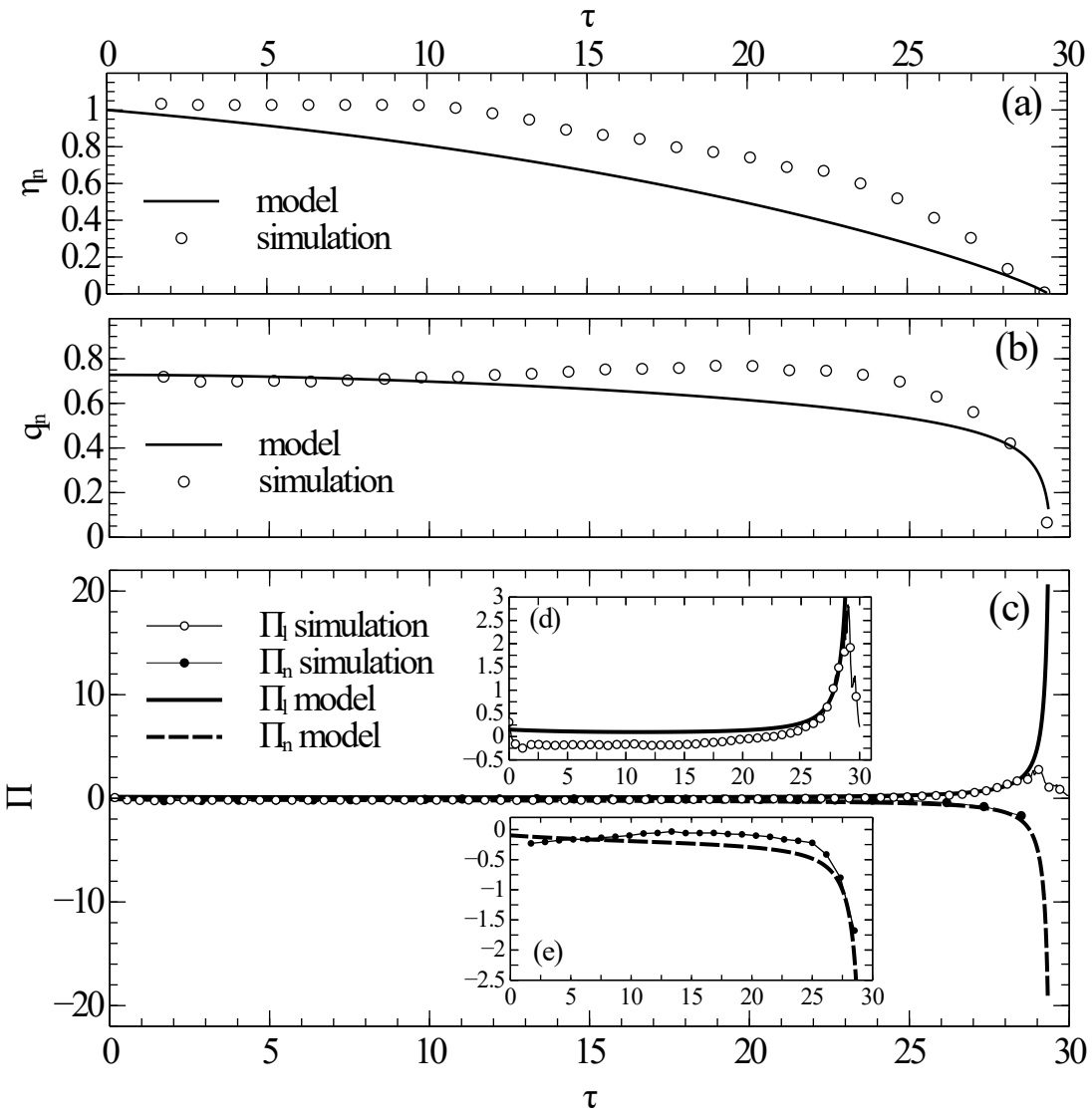

FIG. 5: Results obtained from the model for $\beta = 0.54$, $h = 5.52$, $We = 38.8$ and $\Lambda = 0.147$ with $\alpha = 1.1$ and $\dot{\eta}_n(0) = -0.015$, together with the numerical results corresponding to these values. In particular, temporal evolution of (a) dimensionless neck thickness, (b) dimensionless gas flow through the neck, and (d) dimensionless ligament and neck pressures. Figures (e) and (f) represents a detail of the ligament pressure and the neck pressure, respectively.

a slope close to the experimental one. Nevertheless, the exact values of τ_b are overestimated when the initial neck velocity is set to zero in the model. Consequently, instead of imposing an initial neck velocity equal to zero, $\dot{\eta}_n(0) = 0$, a negative velocity, $\dot{\eta}_n(0) < 0$, to initiate the neck collapse. For this reason, the effect of the initial neck velocity on the bubbling time was investigated next. In particular, for the case of $\beta = 0.52$, $h = 5.27$, $We = 38.26$ and $\Lambda = 0.145$

we found that the bubbling frequency matched the experimental one when $\dot{\eta}_n = -0.019$ was imposed.

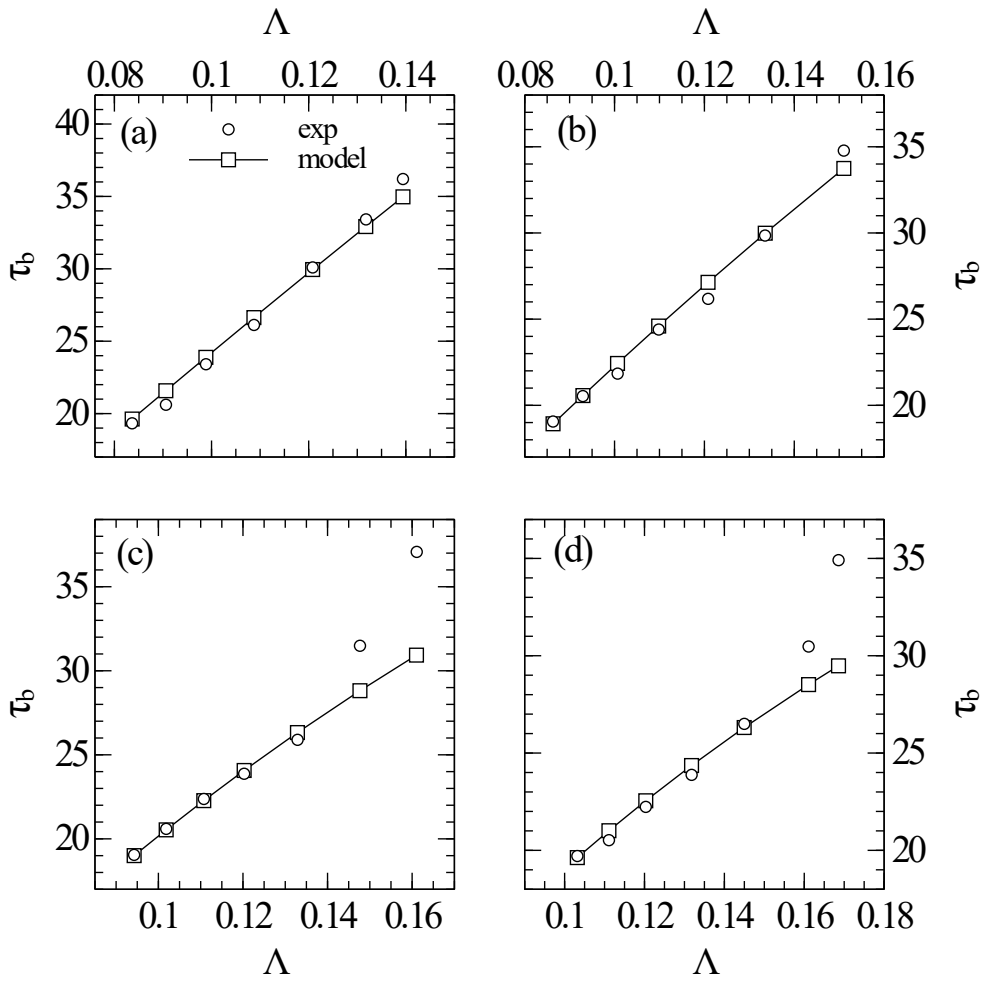

FIG. 6: Bubbling time as a function of the velocity ratio for different values of the Weber number given by the model (squares) with the proper value of the initial neck velocity, (a) $We = 21.528$ m/s, $\dot{\eta}_n(0) = -0.007$ (b) $We = 26.57$, $\dot{\eta}_n(0) = -0.011$ (c) $We = 32.15$, $\dot{\eta}_n(0) = -0.016$, and (d) $We = 38.26$ m/s, $\dot{\eta}_n(0) = -0.019$. Circles are the experimental values reported by Gutiérrez-Montes et al.[9]

Once the appropriate initial neck velocity is imposed, the temporal evolutions of the interface thicknesses, gas flow rate through the neck, and pressures can be compared with the evolutions obtained from the numerical simulations performed by Gutiérrez-Montes et al.[9]. To this aim, we have selected the numerical case closet to the experimental one discussed above, $\beta = 0.54$, $h = 5.52$, $We = 38.8$ and $\Lambda = 0.147$, for which an initial

neck velocity of $\dot{\eta}_n = -0.015$ was found to match the bubbling time obtained numerically, $\tau_b = 29.3$. As observed in Fig. 5, the analytical model matches the numerical results when the appropriate value of $\dot{\eta}_n(0)$ is imposed. In particular, the time evolution of the gas flow rate crossing the neck, $q_n(\tau)$, given by the model closely reproduces the numerical evolution (Fig. 5b). Moreover, it can be noted that, as in the numerical simulations, the model yields a dramatic increase of the ligament pressure, Π_l, previous to the pinch-off, although it is not able to capture the subsequent pressure decrease. In fact, Fig. 5(d) shows that, this initial increase of the ligament pressure closely follows the temporal evolution obtained numerically. Furthermore, the time evolution of the negative neck pressure, Π_n, also agrees with that provided by the numerical simulations, as shown in Figs. 5(c) and (e).

A comparison between the bubbling times provided by the model and those experimentally obtained by Gutiérrez-Montes *et al.*[9] for different values of We and Λ is displayed in Fig. 6. The figure exhibits an excellent agreement between the modeled and the experimental bubbling times once the appropriate initial neck velocity is imposed. Thus, the initial neck velocity needed to reproduce the experimental results has been obtained for different values Λ and We, providing a linear dependence with the Weber number given by $\dot{\eta}_n(0) = 8.4 \times 10^{-3} - 7.3 \times 10^{-4}\,\mathrm{We}$. This expression yields values of $\dot{\eta}_n(0)$ of the order $\mathcal{O}(10^{-2})$ in the range of Weber numbers reported. Although we did not manage to derive an exact model, based on physical arguments, to determine $\dot{\eta}_n(0)$, its order of magnitude can be provided by considering the distance H_o that the neck needs to move during the bubbling time. Thus, using the characteristic bubbling time proposed by Gutiérrez-Montes *et al.*[9], $t_c = H_o/u_a\sqrt{(\rho_w/\rho_a)(h-1)/[\beta(1-\beta)]}$, the neck velocity can be estimated, in dimensional form, as $\dot{h}_n(0) \sim H_o/t_c \sim u_a\sqrt{S\,\beta(1-\beta)/(h-1)}$, where $S = \rho_a/\rho_w$. Consequently, its dimensionless counterpart can be expressed as $\dot{\eta}_n(0) = \dot{h}_n(0)/u_w \sim \sqrt{S\,\beta(1-\beta)/(h-1)}/\Lambda$, which provides $\dot{\eta}_n(0) \sim \mathcal{O}(10^{-2})$ for $\Lambda \sim \mathcal{O}(10^{-1})$.

IV. CONCLUSIONS

A study of the dynamics of the bubbling regime in a system that consists of an air sheet discharging between two co-flowing planar water streams under constant gas flow rate conditions has been performed in this work. Based on previous experimental and numerical results of this problem[9,10], a simple theoretical model able to correctly describe the main

features of the bubbling process has been developed.

The model considers a simplified flow configuration where the bubble interface is divided into three regions, namely, a contraction zone in the neck, a ligament upstream from the neck, and a forming bubble where the air discharges through the neck. The model is one-dimensional, considering that the thicknesses of each region, $h_n(t)$, $h_l(t)$, $h_b(t)$, and their manometric pressures, $p'_n(t)$, $p'_l(t)$, $p'_b(t) = p'_n(t)$, only depend on time. The latter are modeled as a dynamic contribution plus a constant negative pressure caused by the planar expansion that the air finds at the outlet, $p'(t) = p'_d(t) - \rho_a u_a^2 \beta(1-\beta)$, being $\beta = H_i/H_o$ the dimensionless injector wall-thickness. Nevertheless, the pressure loss has been taken into account only inside the neck, since due to the simplicity of the model, it is not possible to include it in both the neck and the ligament simultaneously. With the above assumptions and considering a frame of reference moving at the water velocity, a set of three differential equations for the dimensionless accelerations, $\ddot{\eta}_n$, $\ddot{\eta}_l$, $\ddot{\eta}_b = \ddot{\eta}_n$, is obtained that, together with a pair of algebraic equations for the pressures, Π_n and Π_l, can be integrated to obtain the temporal evolution of the air-water interfaces, pressures, and the gas flow rate through the neck, q_n. The model proposed converges to a final solution when $\eta_b(0) = \eta_l(\tau_b)$, being τ_b the dimensionless bubbling time, using an iterative process.

The model has been evaluated for a particular case, using a zero initial neck velocity, $\dot{\eta}_n(0) = 0$, as a first choice. The results show that the model is able to capture the closure of the neck, the inflation of both the ligament and the forming bubble, as well as the decrease of the gas flow rate through the neck during the final instants, when the pressure inside the ligament increases, and the pressure in the neck falls due to the Venturi effect. Moreover, the bubbling time provided by the model has been obtained for different values of Λ and We, exhibiting trends similar to those obtained experimentally and numerically, although with substantially larger values of τ_b. Therefore, a negative initial neck velocity, $\dot{\eta}_n(0) < 0$, is required to accelerate the initial closure of the neck and match the experimental bubbling time. In fact, the temporal evolution of the interface, gas flow rate through the neck and the neck and ligament pressures given by the model exhibit an excellent agreement with the numerical results when a proper value of $\dot{\eta}_n(0)$ is imposed. This initial neck velocity that matches the bubbling time has been investigated for several values of Λ and We, obtaining that $\dot{\eta}_n(0) \sim \mathcal{O}(10^{-2})$, an order of magnitude that can be estimated using the characteristic

break-up time proposed by Gutiérrez-Montes et al.[9] for the same configuration. In particular, within the parameter ranges investigated herein, the value of initial velocity has been found to decrease linearly with We as $\dot{\eta}_n(0) = -7.3 \times 10^{-4} We + 8.4 \times 10^{-3}$.

---

[1] Bolaños-Jiménez, R., Sevilla, A., Gutiérrez-Montes, C., Sanmiguel-Rojas, E., Martínez-Bazán, C., 2011. Bubbling and jetting regimes in planar coflowing air-water sheets. J. Fluid Mech. 682, 519–542.

[2] Bolaños-Jiménez, R., Sevilla, A., Martínez-Bazán, C., Gordillo, J. M., 2008. Axisymmetric bubble collapse in a quiescent liquid pool. Part II: Experimental study. Phys. Fluids 20, 112104.

[3] Chuang, S. C., Goldschmidt, V. W., 1970. Bubble formation due to a submerged capillary tube in quiescent and coflowing streams. Trans. ASME D: J. Basic Engng 92, 705–711.

[4] Davidson, J. F., Schuler, B. O. G., 1960. Bubble formation at an orifice in an inviscid liquid. Trans. Instn. Chem. Engrs. 38, 335–342.

[5] Gordillo, J. M., Cheng, Z., Márquez, M., Gañán Calvo, A. M., Weitz, D. A., 2004. A new device for the generation of microbubbles. Physics of Fluids 16, 2828–2834.

[6] Gordillo, J. M., Gañán-Calvo, A. M., Pérez-Saborid, M., 2001. Monodisperse microbubbling: Absolute instabilities in coflowing gas-liquid jets. Phys. Fluids 13, 3839–3842.

[7] Gordillo, J. M., Sevilla, A., Martínez-Bazán, C., 2007. Bubbling in a coflow at high Reynolds numbers. Phys. Fluids 19, 077102.

[8] Gordillo, J. M., Sevilla, A., Rodríguez-Rodríguez, J., Martínez-Bazán, C., 2005. Axisymmetric bubble pinch-off at high Reynolds numbers. Phys. Rev. Lett. 95, 194501.

[9] Gutiérrez-Montes, C., Bolaños-Jiménez, R., Sevilla, A., Martínez-Bazán, C., 2013. Experimental and numerical study of the periodic bubbling regime in planar co-flowing airwater sheets. Int. J. Multiphase Flow 50, 106–119.

[10] Gutiérrez-Montes, C., Bolaños-Jiménez, R., Sevilla, A., Martínez-Bazán, C., 2014. Bubble formation in a planar water–air–water jet: Effects of the nozzle geometry and the injection conditions. Int. J. Multiphase Flow 65, 38–50.

[11] Kulkarni, A. A., Joshi, J. B., 2005. Bubble formation and bubble rise velocity in gas-liquid systems: A review. Ind. Eng. Chem. Res. 44 (16), 5873–5931.

[12] Kumar, R., Kuloor, N. R., 1976. The formation of bubbles and drops. Chem. Engng. Sci. 31, 453.

[13] Longuet-Higgins, M. S., Kerman, B. R., Lunde, K., 1991. The release of air bubbles from an

underwater nozzle. J. Fluid Mech. 230, 365–390.

[14] Maier, C. G., 1927. U. S. Bur. Mines Bull. 260.

[15] Marmur, A., Rubin, E., 1970. A theoretical model for bubble formation at an orifice submerged in an inviscid liquid. Adv. Chem. Engng 8, 256–368.

[16] Oğuz, H. N., Prosperetti, A., 1993. Dynamics of bubble growth and detachment from a needle. J. Fluid Mech. 257, 111–145.

[17] Ramakrishnan, R., Kumar, R., Kuloor, N. R., 1968. Studies in bubble formation I: Bubble formation under constant flow conditions. Chem. Eng. Sci. 24, 731.

[18] Rodríguez-Rodrıguez, J., Sevilla, A., Martínez-Bazán, C., Gordillo, J., 2015. Generation of microbubbles with applications to industry and medicine. Annu. Rev. Fluid Mech. 47, 405–429.

[19] Sevilla, A., Gordillo, J. M., Martínez-Bazán, C., 2002. The effect of the diameter ratio on the absolute and convective instability of free coflowing jets. Phys. Fluids 14, 3028–3038.

[20] Sevilla, A., Gordillo, J. M., Martínez-Bazán, C., 2005. Bubble formation in a coflowing air-water stream. J. Fluid Mech. 530, 181–195.

[21] Sevilla, A., Gordillo, J. M., Martínez-Bazán, C., 2005. Transition from bubbling to jetting in a coaxial air-water jet. Phys. Fluids 17, 018105.

[22] Stone, H. A., Strook, A. D., Adjari, A., 2004. Engineering flows in small devices: Microfluidics toward a lab-on-a-chip. Ann. Rev. Fluid Mech. 36, 381–411.

[23] Tan, R. B. H., Harris, I. J., 1986. A model for non-spherical bubble growth at a single orifice. Chem. Engng Sci. 41, 3175.

[24] Terasaka, K., Tsuge, H., 1993. Bubble formation under constant flow conditions. Chem. Engng Sci. 48, 3417–3422.